IEICE Proceeding Series

Synchronization in networks of excitable elements with time-delayed and rectifying coupling

Sten Rüdiger, Ronny Möbius, Lutz Schimansky-Geier

Vol. 1 pp. 555-558
Publication Date: 2014/03/17
Online ISSN: 2188-5079

2012 International Symposium on Nonlinear Theory and its Applications
NOLTA2012, Palma, Majorca, Spain, October 22-26, 2012

Synchronization in networks of excitable elements with time-delayed and rectifying coupling

Sten Rüdiger, Ronny Möbius and Lutz Schimansky-Geier

Institut für Physik, Humboldt-Universität zu Berlin, Germany
Email: sten.ruediger@physik.hu-berlin.de

Abstract—We study the synchronization properties of excitable FitzHugh-Nagumo elements in a one-dimensional network. Elements are coupled to their nearest neighbors with a stimulating, or rectifying, term with time delay. We first show how time delay can be obtained for networks of coupled neurons. States of global synchronization in the network are analyzed by bifurcation theory. We then consider spatial aspects of the synchronization by direct simulation for fixed and distributed delay times and characterize the effect on the shape of excitation spikes. We find that for distributed delays, echo pulses appear and meander and are of arbitrary duration, whereas for non-distributed delay they are fixed and of constant duration.

1. Introduction

Coupling of nonlinear dynamical equations by delay is a widely used modeling approach for phenomena as for example laser systems [1] and neuronal communication [2, 3]. In [4] we compared dynamical behaviors of arrays of excitable elements according to the nature of the coupling, either diffusive or time-delayed. In the case of time-delayed coupling, signals from neighboring elements were shown to serve as mutual excitations, resulting in a prolonged duration of the excitation. In this analysis local dynamics was described by a FitzHugh-Nagumo-type model.

Later we considered genuinely spatial structures by allowing for large domains and translation of excitatory spikes through the domain [5]. There we described the effects of delay-coupling on the properties of pulse solutions such as their propagation speed as well as pulse shape. Propagation of pulses is an important aspect of pattern-forming systems, which is for our system inherited from the standard diffusively coupled equations and preserved for small delays. As the delay time is increased, propagating pulses undergo a transition in their spatial shape. Finally, in the case of large delay times, a transition to a stationary and spatially coherent regime occurs.

Here we first give a derivation of the special delay coupling term, which extends the motivation we have been given earlier [4]. Then we describe our findings on existence and stability of simple space-filling solutions and the complex pulse solutions in 1D that exist in a certain range of the parameter space. We finally present recent simulations of one-dimensional arrays where the delay times are randomly distributed.

2. Derivation of model equations with time-delayed coupling

Coupling to neighbors with delay has frequently been studied in models for collective neural activity. In neurons, delay results from different processes, such as synaptic delay or transmission delay. Delay was studied in the frame-work of continuous neural fields, where it results in the interaction function in a distance-dependent manner [2]. The effects of delay have also frequently been incorporated into integrate-and-fire networks [6, 7]. It is much less studied, however, which effects delay-coupling enforces in networks of excitable elements.

Coupling with delay can be mathematically derived for integro-differential equations, which occur for instance in models for neural waves [8]. We may start using a simple neural field model,

$$\begin{aligned}\frac{\partial v(x,t)}{\partial t} &= f(v(x,t)) \\ &+ \int_D J(y-x) \left[v\left(y, t - \frac{|x-y|}{u}\right) - 1 \right] dy\end{aligned}$$

where $v(x,t)$ denotes the firing rate of the cells. $J(x)$ is an even interconnection function of neurons and is assumed to have a strongly localized maximum at $x = 0$ and to vanish for $x \to \pm\infty$. The term $v(y, t - \frac{|x-y|}{u}) - 1$ mediates the impact of deviations from the standard firing rate $v = 1$ on neighboring neurons. Since a signal travels along the output link, i.e. the axon, with finite velocity u, the signal arrives after time delay $|x-y|/u$. In one dimension and after a variable substitution, we have

$$\begin{aligned}\frac{\partial v(x,t)}{\partial t} &= f(v(x,t)) \\ &+ \int_{-\infty}^{+\infty} J(z) \left[v\left(x-z, t - \frac{|z|}{u}\right) - 1 \right] dz.\end{aligned}$$

Next, we discretize $v(x,t)$ and the integral by considering that neurons are placed at distances Δx from each other,

$$\begin{aligned}\frac{\partial v_i(t)}{\partial t} &= f(v_i(t)) \\ &+ \sum_j \Delta x J(j\Delta x) \left[v_{i-j}\left(t - \frac{j\Delta x}{u}\right) - 1 \right],\end{aligned}$$

where $v_i(t)$ is the value of $v(x,t)$ at position $i\Delta x$. Since $J(x)$ is assumed to be strongly localized, we neglect all input neurons except for the nearest ones to obtain

$$\begin{aligned}\dot{v}_i &= f(v_i) + \Delta x J(0)(v_i(t) - 1) \\ &\quad + \Delta x J(\Delta x)(v_{i+1}(t - \Delta x/u) - 1) \\ &\quad + \Delta x J(\Delta x)(v_{i-1}(t - \Delta x/u) - 1) \\ &= f(v_i) - \Delta x J(0) - 2c + (2c + \Delta x J(0))v_i(t) \\ &\quad + c(v_{i-1}(t-\tau) + v_{i+1}(t-\tau) - 2v_i(t)),\end{aligned}$$

where $\tau = \Delta x/u$ characterizes the time delay and the last terms could be seen as resembling a diffusive coupling of strength $c = \Delta x J(\Delta x)$. The last equation has been cast in a form clearly distinguishing the local firing dynamics from the interaction, which is diffusive in the case of $\tau = 0$.

Here we explicitly consider networks of FitzHugh-Nagumo (FHN) elements that are coupled to neighbors by delay-diffusive terms in the manner just described. The model consists of a system of N FHN elements that are coupled with time delay in the activator variable. If one considers periodic boundary conditions, the system may be thought as an infinite chain or a ring of FHN elements. The set of equations is

$$\frac{\partial v_i}{\partial t} = v_i(1 - v_i)(v_i - a) - w_i - w_0 + C_i, \quad (1)$$

$$\frac{\partial w_i}{\partial t} = \epsilon(v_i - \gamma w_i). \quad (2)$$

Here, v_i and w_i denote the activator and inhibitor variable, respectively, of element i, where i = 1,...,N. In view of the motivation given above, v_i represents the firing function with self-activating local dynamics, while w_i is a further quantity representing inhibiting physiological processes.

C denotes the coupling and is given by

$$\begin{aligned}C_i &= c\,\mathrm{Max}(0, v_{i-1}(t-\tau) - v_i(t)) \\ &\quad + c\,\mathrm{Max}(0, v_{i+1}(t-\tau) - v_i(t)).\end{aligned} \quad (3)$$

At $i = 1, N$ we employ periodic conditions, such that element 1 is coupled to element N. In difference to the kind of systems that were discussed in the previous paragraphs, we have added a maximum function in the coupling term. The purpose of the maximum value function is to ensure not to have a negative value for the coupling. It thus acts similar to a diode, allowing only stimulating or excitatory signals on neighbors. An exclusively excitatory coupling may be expected for neurons, which are frequently assumed to enter an excited state upon passing a voltage threshold by input from connected neurons.

Eq. (3) is a non-differentiable right-hand-side of differential equations (1). In the language of dynamical systems, the equations are non-smooth yet continuous [9]. In the non-smooth case, special care has to be taken when studying the equations' dynamics, particularly the stability and bifurcations of fixed-points. However, conditions for local bifurcations based on eigenvalues can be generalized in a straight-forward way. Indeed, we found that instabilities of fixed points are not relevant for the dynamics we observe in simulations. Instead we analyze bifurcations of periodic orbits, where standard bifurcation theory can be extended to non-smooth continuous systems.

The small ϵ parameter (here chosen at $\epsilon = 0.01$) enforces that the inhibitor variables w_i functions on a much slower timescale than the activator variables v_i. Our choice of the two parameters $a = 0.1$ and $w_0 = -0.1$ puts the system on the edge of excitability, i.e., the system possesses a stable fixed point where all elements reside at (v^*, w^*), but sufficiently large perturbations away from this fixed point will lead to a large excursion in phase space.

3. Linear stability and bifurcation analysis

The bifurcation scenario for simple solutions of two coupled elements will be discussed first. For our set of parameters, we did not find any numerical evidence of a coupling-induced instability of the trivial state, ie., the fixed-point solution $v_i = v_*,\ w_i = w_*$. However, in our direct numerical simulations we have found that periodic solutions, characterized by a phase shift of half of their period between adjacent elements, are a very robust appearance[5].

To elucidate the origin of periodic, anti-phase solutions, their branching behavior is of interest. Because of the spatial periodicity of anti-phase solutions, they can be considered as stable, temporal oscillations of two coupled elements. The equations we studied are those in Eqs. (1,2) with $N = 2$. We used the branch-continuation software DDE-BIFTOOL [10] to determine the range of existence and stability of the periodic anti-phase orbit.

As suggested by our numerical simulations, we found a family of stabilized non-trivial solutions with the characteristic feature of anti-phase oscillation [5]. A branch of periodic orbits was then followed in τ for fixed c and turned out to be connected with a branch of periodic orbits of smaller amplitude. Both branches collide in saddle-node bifurcation at small τ, such that a threshold in delay times τ exists, below which no periodic orbit occurs. For smaller c we also found further saddle-node bifurcation of the periodic orbits. Islands of periodic solutions exist at small coupling strength. If c is increased, the island at $\tau \approx 40$ is connected to the solutions at $\tau \approx 70$. Similarly, further numerical analysis showed that at larger τ additional islands exists (if c is small).

The two branches produced in a saddle-node bifurcation generally have different stability properties. We found that the lower branch is always unstable, while the upper branch looses stability by a pitchfork bifurcation. These result can be summarized to the bifurcation diagram shown in Fig. 1. Stable periodic solutions only exists above and to the right of the solid curve. Particularly, for $c = 0.3$ we obtain a minimal τ for the existence of periodic solutions of around 17, consistent with the onset of stationary antiphase oscillations shown in Section 4. For comparison we have

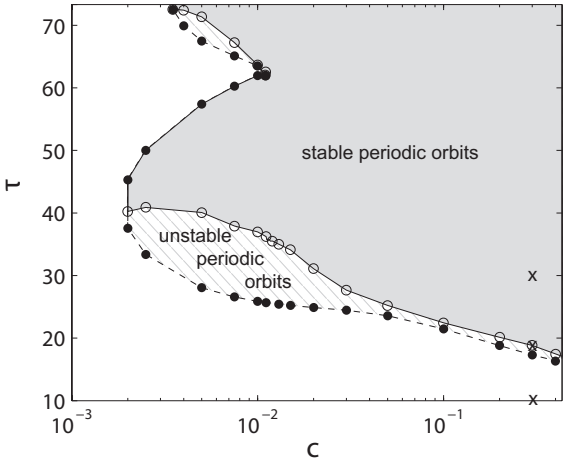

Figure 1: Location of saddle-node bifurcation (filled circles) and pitchfork bifurcation (open circles) of antiphase oscillations in parameter space. Stable periodic orbits exist to the right and above the solid lines. Crosses show the location of parameters for simulations shown in Fig. 2 A,B, and C (from bottom to top).

added crosses in Fig. 1 to represent the simulations shown in Fig. 2.

The islands are limited by saddle-node bifurcations (filled circles) and lead to the folds on the left boundary in Fig. 1. Areas between the solid and dashed lines contain unstable periodic orbits, which become stabilized by pitchfork bifurcations (open circles). Note that in the entire parameter space the fixed point is also stable leading to bistability of fixed point and periodic solution.

4. Simulations of 1D arrays of excitable elements

We now examine solutions using direct numerical simulation in a one-dimensional array of $N = 100$ excitable elements. Typical space-time plots are shown in Fig. 2. In the following we hold the parameter c fixed at 0.3 and vary the delay time τ. Like in many other locally excitable system, diffusive coupling leads to the existence of uniformly translating solutions for small delay times [11]. The localized perturbation propagates along the spatial coordinate and acquires a fixed shape with a certain spatial extension. A typical pulse-like solution is shown in Fig. 2A.

For large time delay anti-phase oscillations appear, which form a checker pattern in a space-time plot (Fig. 2C). Because of their spatial periodicity, these solutions correspond to the anti-phase oscillations described in the previous section.

In a further regime with intermediate delay times we found antiphase oscillations with defects frozen into the pattern (echo waves, Fig. 2B). This regime was described in [5] to bridge the simple pulse solutions for small τ with the sustained anti-phase oscillations found for larger τ. The defects resemble the echo waves described in [5] where echo-

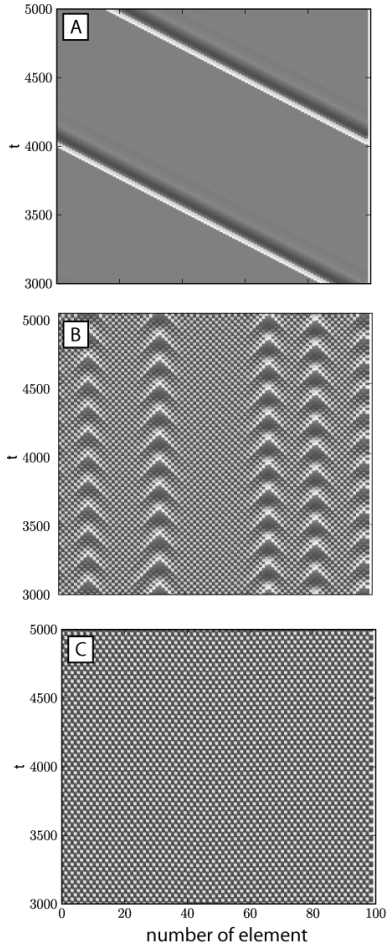

Figure 2: Space-time plots of the v-component, from top to bottom: standard pulse $\tau = 10$ (A), echo pulses $\tau = 19$ (B), antiphase oscillations $\tau = 30$ (C, for all runs $c = 0.3$)

ing from the neighboring elements makes the element spike again with diminished amplitude after a normal excitation.

It is interesting to note that these echo states can be stabilized at fixed positions in the domain. Here the echo waves are periodically generated and annihilated in a localized manner. In contrast, in our earlier simulations in [5] we had added noise and found that the defects are unlocked from their fixed position.

5. Simulations with distributed delays

We finally present simulations for 1D lattices where the delay times have been chosen from a random distribution, ie., we now employ a coupling term

$$\begin{aligned} C_i &= c\,\mathrm{Max}(0, v_{i-1}(t-\tau_i^-) - v_i(t)) \\ &\quad + c\,\mathrm{Max}(0, v_{i+1}(t-\tau_i^+) - v_i(t)). \end{aligned} \tag{4}$$

The delay times $\tau_i^{\pm}$ have been chosen from a Poisson distribution with mean $\bar{\tau}$ and kept fixed throughout the simulation run.

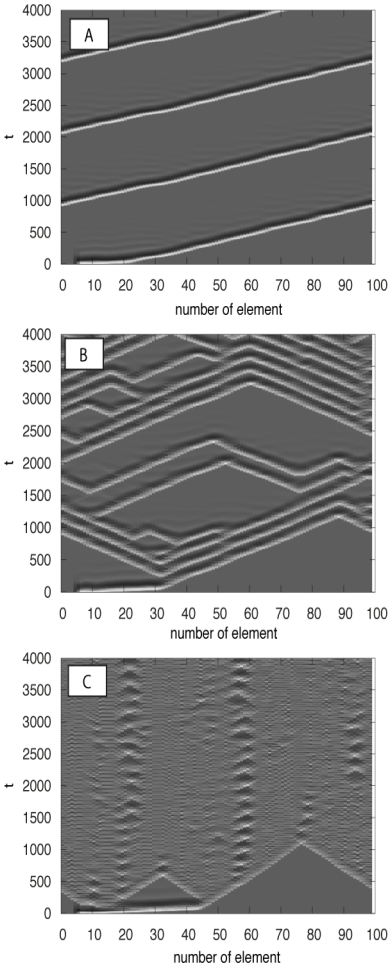

Figure 3: Simulations with delay times τ at each link chosen from a distribution with mean $\bar{\tau} = 10, 19, 30$ (A,B, and C, resp.). It can be seen that echo pulses can be meandering through the domain for $\tau = 19$ (B), while for larger delay time they are frozen into the pattern (C).

Fig. 3 shows three exemplary simulation for the same $\bar{\tau}$ values as in Fig. 2. For small $\bar{\tau}$ the pulse solutions are very similar to the case of fixed delay time (Fig. 3A). The main difference to the case of fixed delay time is the generation of irregular pulse dynamics in the case of intermediate τ. While for fixed τ defects are frozen into the background pattern of antiphase oscillations (Fig. 2B) , we here find that the pulses can be compelled to move towards both directions and as well that two pulses in opposite directions can annihilate. The pattern shares some qualitative features with those for a forced complex Ginzburg-Landau equation [12].

Finally for large delay time antiphase oscillations with defect solutions appear (Fig. 3C). These patterns again resemble the patterns for smaller fixed τ (Fig. 2B) but with fluctuating appearance of the defects.

6. Summary

Our analysis of delay-coupled excitable dynamics has revealed a rich repertoire of spatio-temporal patterns. The simplest solutions, antiphase oscillations of the entire domain, can be studied by bifurcation analysis. While those solutions exist for large delay time, we found an interesting regime of echo waves for intermediate delay times. Echo waves are characterized by a second time scale, which is much longer than the original time scale of the excitable system and is not present in standard diffusively coupled systems. Recently we have analyzed arrays with randomly distributed delay times. The delay times were chosen in the beginning of each simulation according to a Poisson distribution. We found that the quenched noise generates an irregular spatio-temporal dynamics of echo waves.

References

[1] Appeltant L. et al., Nature Communications *2*, 468 (2011).

[2] Hutt, A., Bestehorn, M., Wennekers, Network: Computation in Neural Systems **14**, 351–368 (2003).

[3] Sethia, G.C. and Sen, A. and Atay, F.M., Physical Review E 81: 056213 (2010).

[4] Rüdiger, S., Schimansky-Geier, L., J. Theor. Biol. **259**, 96-100 (2009).

[5] O. Valles, R. Möbius, S. Rüdiger, L. Schimansky-Geier Phys. Rev. E 83, 036209 (2011).

[6] Golomb, G., Ermentrout, G.B., Network: Comput. Neural Syst. **11** 221 (2000).

[7] Haken, H., Eur. Phys. J. B **18**, 545 (2000).

[8] Murray, J.D., Mathematical Biology: Spatial models and biomedical applications, Springer Verlag (2003).

[9] R. I. Leine, H. Nijmeijer, *Dynamics and Bifurcations of Non-Smooth Mechanical Systems*, Springer Verlag, Berlin, 2004.

[10] Engelborghs, Luzyanina, K. T., Roose, D., ACM Transactions on Mathematical Software, **28**, 1 (2002).

[11] Hizanidis, J., et al., Phys. Rev. Lett. **96**, 244104 (2006),

[12] Pikovsky, A., Rosenblum M., Kurths, J., *Synchronization, A universal concept in nonlinear science*, 2001.